Polysaccharide Microcrystals Reinforced Amorphous Poly(β-hydroxyoctanoate) Nanocomposite Materials

David Dubief, Eric Samain, and Alain Dufresne*

Centre de Recherches sur les Macromolécules Végétales (CERMAV-CNRS), Université Joseph Fourier, BP 53, 38041 Grenoble, Cedex 9, France

Received February 24, 1999; Revised Manuscript Received June 9, 1999

ABSTRACT: In a previous work [*Macromolecules* **1998**, *31*, 6426] the preparation technique of a latex of poly(β-hydroxyoctanoate) (PHO) obtained from *Pseudomonas oleovorans* grown at high cell density on sodium octanoate was presented. The resulting films displayed typical properties of thermoplastic elastomer. Depending on the experimental purification conditions, fully amorphous PHO films can be obtained. Nanocomposite materials were prepared using this latex as a matrix and using a colloidal suspension of hydrolyzed starch or cellulose whiskers as a natural and biodegradable filler. After stirring, the preparations were either cast and evaporated or freeze-dried and molded. High-performance materials were obtained from these systems, preserving the natural character of PHO. The resulting properties were strongly related to the aspect ratio L/d (L being the length and d the diameter) of the filler and to the geometric and mechanical percolation effects. In addition, specific polymer−filler interactions and geometrical constraint due to the particle size of the latex have to be considered to account for the mechanical reinforcement effect of cellulose whiskers.

Introduction

Poly(hydroxyalkanoates) (PHAs) are biopolymers stored in intracellular inclusion bodies by a wide variety of bacteria as an energy reserve.[1−3] PHAs are thermoplastic materials, and in contrast to synthetic polymers, they have the fundamental advantage of being renewable resources not dependent on the supply of petroleum.

The most common PHA is poly(β-hydroxybutyrate) (PHB), a highly crystalline and brittle thermoplastic. In contrast, poly(β-hydroxyoctanoate) (PHO) is a polyester containing a long pendant group in each repeat unit[4−9] and has the properties of a thermoplastic elastomer.[10−12] It is produced by *Pseudomonas oleovorans*, which grows on sodium octanoate or octane as the carbon source under a limited nutrient or a lack of oxygen condition.

Three major procedures for the separation of PHA from bacteria cells exist: solvent extraction, chemical digestion, and selective enzymolysis.[13] The two latter methods consist of selective removal of non-PHA components, and these methods can preserve the nascent state and the granular morphology of PHA, allowing more diverse applications than solvent-extracted PHA. A separation procedure, using differential digestion with sodium hypochlorite to separate bacterial biomass from PHB, was described by Williamson and Wilkinson.[14] Although simple and effective, this method has been avoided because it has been reported to cause severe degradation of the PHB molecular weight.[15−17] In a previous work,[18] a chemical treatment by sodium hypochlorite was used to prepare a latex of PHO. Cell suspensions were treated with different amounts of sodium hypochlorite to purify the PHO. It was reported that optimal conditions for the bacteria digestion corresponded to a hypochlorite concentration between 21 and 26 mmol of NaOCl/g of biomass. Lower hypochlorite

concentration resulted in a decrease in the polymer purity. At higher hypochlorite concentration, a coalescence of PHA granules was observed during the purification process, due to the removal of murein sacculus.[18] It was shown that the stabilization of the latex occurred spontaneously without any surfactant due to the persistence around the polymer granules of the murein sacculus. In contrast to what was observed in the literature with PHB, no significant degradation of the polymer was reported after this purification procedure.[18]

Polymer aqueous suspensions, or latices, have generated great interest due to their industrial applications as films, coatings, and blends with other polymers. It is also possible to prepare composites by mixing different types of water suspensions, including some polymer latices and organic or inorganic stabilized suspensions. Materials can be easily processed, either by film-casting techniques (water evaporation) or by freeze-drying followed by a classical extrusion process. Previous works performed in our laboratory deal with the processing and the characterization of nanocomposite materials with a synthetic polymeric latex as a matrix reinforced by cellulose whiskers[19−21] or starch microcrystals.[22,23] When the former are homogeneously dispersed into polymer matrices, they give a remarkable reinforcing effect, even at concentrations of a few percent. Moreover, using an amorphous matrix and because of their size, the cellulose or starch microcrystals enable the production of highly filled transparent films. The latter are particularly attractive available and renewable fillers, which reinforce the polymer matrix[22,23] and can be used as a low-value material into PHA formulations.

The aim of the present paper is to process and characterize natural nanocomposite materials using PHO latex as matrix and polysaccharide fillers, like starch microcrystals, or cellulose whiskers as the reinforcing phase.

Experimental Section

PHO Latex Preparation. The bacterial strain and growth conditions of *Pseudomonas oleovorans* (ATCC 29347) were

* To whom correspondence should be addressed. e-mail: dufresne@cermav.cnrs.fr.

described elsewhere.[18] In the present work, a hypochlorite concentration of 21 mmol of NaOCl/g of biomass was used. The time required to treat PHO granules was fixed at 5 h in this study. The average diameter of PHO particles in the latex was around 1 μm, which corresponds to the in vivo inclusion dimension.[18] The typical monomer composition of PHA produced by sodium octanoate grown cells has already been described.[5] *Pseudomonas oleovorans* produces a random copolymer composed of mostly C8 and smaller amounts of C6 and C10 monomers when fed on octanoate. The octanoate content was shown to be about 86%. In addition, it was reported that changing growth conditions did not have a significant influence on the monomer composition of the PHA produced with sodium octanoate.[24]

Prior to chemical digestion with sodium hypochlorite, bacteria were either freeze-dried (PHO$_{FD}$) as in the earlier study[18] or simply frozen (PHO$_F$) and stored at -20 °C.

Polysaccharide Fillers. To vary the aspect ratio, polysaccharide microcrystals were obtained from both starch and cellulose. They were prepared by acid hydrolysis of amorphous domains of either smooth yellow pea granules (COSUCRA, Fontenoy, Belgium) or tunicin, an animal cellulose extracted from tunicate, whose microfibrils are particularly well organized and therefore highly crystalline. Colloidal suspensions in water were prepared as described elsewhere.[19,22] Smooth yellow pea starch microcrystals are a few tens of nanometers in diameter, and their aspect ratio, L/d (L being the length and d the diameter of the filler) is assumed to be close to 1, as reported elsewhere for potato starch microcrystals.[22] Tunicin whiskers consist of parallelepiped rods with the length ranging from 100 nm to several micrometers (average value around 1 μm) for widths on the order of $10-20$ nm.[19] The aspect ratio of these whiskers was estimated from transmission electron microscopy and was around 67.

Film Processing. The PHO granule suspensions were purified by 15 h dialysis against distilled water. The colloidal microcrystalline suspension (starch or cellulose) was mixed with the PHO granule suspension at different ratios in order to obtain composite films with a good level of dispersion and with different compositions. Composite materials were processed using only PHO$_F$ as a matrix. The starch microcrystal loading was varied from 0 to 50 wt % and the cellulose microcrystals loading from 0 to 6 wt %. After stirring, the air in the suspension was removed by vacuum prior to casting in a Teflon mold (2×7 mm). Films were obtained by storing the casting at 35 °C to allow water evaporation and polymer particle coalescence.

Along this study, the achieved results will be compared to those observed with model systems processed using a latex obtained by the copolymerization of styrene (34 wt %) and butyl acrylate (64 wt %) containing 1% acrylic acid and 1% acrylamide, provided by Elf-Atochem (Serquigny, France).[19,22,23] The aqueous suspension of poly(styrene-*co*-butyl acrylate) (poly(S-*co*-BuA)) contained spherical particles with an average diameter around 150 nm, and the glass−rubber transition temperature (T_g) of the copolymer was around 0 °C.

Differential Scanning Calorimetry. Differential scanning calorimetry (DSC) was performed with a Perkin-Elmer DSC7, fitted with a cooler system using liquid nitrogen. It was calibrated with an indium standard and operated at a heating rate of 15 K/min. Scans were performed from -60 to $+80$ °C on samples ($\sim$10 mg) at least 2 weeks after film formation to ensure stabilization of the degree of crystallinity and perfect reliability of measurements.

X-ray Diffraction. Wide-angle X-ray scattering (WAXS) patterns were measured in reflection with a diffractometer using a static detector (Siemens D500). Samples were mounted on a support and exposed for a period of 10 s for each angle of incidence using a Cu Kα_1 X-ray source with a wavelength of 1.5406 Å operating at 40 kV and 20 mA. The angle of incidence was varied between 3° and 30° by steps of 0.04°. WAXS patterns were recorded at several time intervals after film formation to ensure perfect reliability of measurements and to detect any possible evolution of the material with time.

Karl Fischer Titration Analysis. The Karl Fischer titration apparatus (Metrohm model 684) employed in this study consisted of a moisture-protected buret system of conventional design.[25] The titration flask itself was provided with a sidearm ground joint for the addition of samples to be titrated. Dry nitrogen gas was supplied through a bypass arrangement on the sidearm to prevent introduction of atmospheric moisture. The method consists of measuring the change of conductance between two platinum electrodes inserted into the titration flask. The Karl Fischer reagent used in this study was the one proposed by Swensen and Keyworth,[26] which global reaction is

$$I_2 + SO_2 + 3C_5H_5N + HCONH_2 + H_2O \rightarrow$$
$$C_5H_5N,HSO_3NHCHO + 2C_5H_5N,HI$$
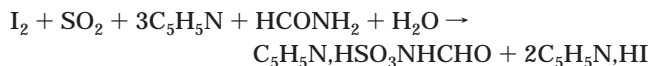
Molecular Weight Measurements. Number-average molecular weight, $\bar{M}_n$, weight-average molecular weight, $\bar{M}_w$, and polydispersity index $\bar{M}_w/\bar{M}_n$ were determined by size exclusion chromatography (SEC) with a Waters apparatus (510 pump), using a set of four columns (Styragel HR0.5, HR1, HR2, and HR5) and tetrahydrofuran with a flow rate of 1.1 mL min^{-1}. A refractive index detector (Waters 410) was used for detection. For calibration, polystyrene standard solutions were injected.

Scanning Electron Microscopy. Scanning electron microscopy (SEM) was performed to investigate the morphology of the materials with a JEOL JSM-6100 instrument. The specimens were frozen under liquid nitrogen, then fractured, mounted, coated with gold on a JEOL JFC-1100E ion sputter coater, and observed. SEM micrographs were obtained using 7 kV secondary electrons.

Dynamic Mechanical Analysis. Dynamic mechanical tests were carried out with a Rheometrics RSA2 spectrometer in the tensile mode. Test conditions were chosen in such a way that the measurements were in the linear viscoelasticity region (the maximum strain ϵ was around 10^{-4}). The specimen was a thin rectangular strip with dimensions of $30 \times 3 \times 1$ mm. Measurements were performed in isochronal conditions at 1 Hz, and the temperature was varied by steps of 3 K.

Results and Discussion

Characterization of the PHO Matrix. The characterization of the PHO film resulting from the coalescence of the PHO latex obtained from freeze-dried bacteria treated with sodium hypochlorite (PHO$_{FD}$) was presented elsewhere.[18] It was shown that the crystallinity increased at room temperature with time after film formation. It displayed typical properties of thermoplastic elastomer. After 2 weeks, the crystallinity did not change further.

Wide-angle X-ray scattering (WAXS) was used to characterize PHO films obtained from latices purified by sodium hypochlorite using either freeze-dried (PHO$_{FD}$) or frozen (PHO$_F$) bacteria (Figure 1). The amorphous part of PHO$_{FD}$ was characterized by a broad hump located around $2\theta = 20°$, whereas the crystalline zones displayed three diffraction peaks near 5°, 20°, and 22°, as reported earlier.[18] The melting and glass transition temperatures were determined from DSC experiments and were found around 55 and -36 °C, respectively. These values agree with what was reported in the literature.[11]

In contrast, the polymer extracted from frozen bacteria showed no diffraction peak and displayed typical behavior of a fully amorphous polymer. As well, DSC did not display any melting point, even for longer aging times at room temperature. Compared to the semicrystalline polymer (PHO$_{FD}$), no significant difference was
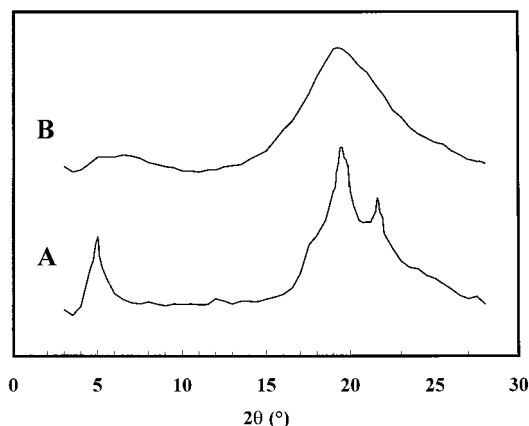
Figure 1. Wide-angle X-ray diffraction patterns for PHO films obtained from latices purified by sodium hypochlorite using either freeze-dried (A) or frozen (B) bacteria.
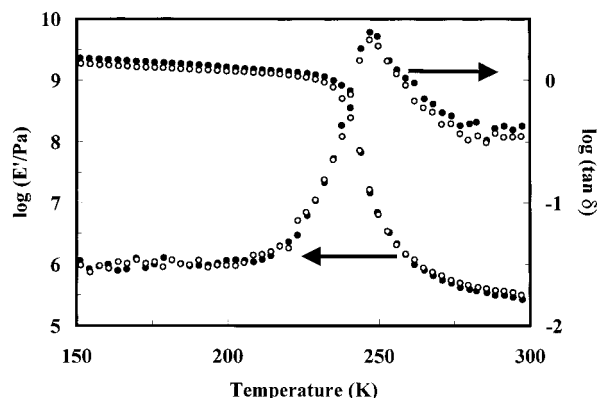

Figure 2. Dynamic mechanical behavior of PHO_F films: logarithm of the storage tensile modulus E' and logarithm of the loss angle tangent tan δ versus temperature at 1 Hz for the PHO film obtained from the coalescence of PHO_F after (●) 0 and (○) 2 weeks annealing times at room temperature after film formation.

Figure 3. Kinetic of water loss: residual water content versus time for PHO films obtained from the coalescence of polymer granules extracted by sodium hypochlorite of (●) freeze-dried and (○) frozen bacteria. (The solid lines serve to guide the eye.)

Table 1. Number-Average Molecular Weight, $\bar{M}_n$, Weight-Average Molecular Weight, $\bar{M}_w$, and Polydispersity Index $\bar{M}_w/\bar{M}_n$ of PHO Obtained from Freeze-Dried Bacteria (PHO_{FD}) and Frozen Bacteria (PHO_F)

sample	$\bar{M}_n$ (10^3 g mol^{-1})	$\bar{M}_w$ (10^3 g mol^{-1})	$\bar{M}_w/\bar{M}_n$
PHO_{FD}	78.7	156.7	1.99
PHO_F	54.4	150.8	2.77

weak plasticizer for PHB, changing the glass transition, in the case of P(HB-co-8% HV), from 4 °C without water to −3 °C with water. The residual water content was low in the PHO films prepared in this study, regardless of the state of the bacteria prior to the purification step (Figure 3). The film obtained from PHO_{FD} was semicrystalline and had a higher water content (∼1.1 wt %), whereas the one obtained from PHO_F was amorphous and had a lower water content (∼0.8 wt %). Therefore, the difference in residual water content between the two systems was slight, and in addition, there was no difference in the T_g value (−36 and −37 °C, respectively).

Size exclusion chromatography (SEC) was also performed to characterize the molecular weight of PHO_{FD} and PHO_F (Table 1). $\bar{M}_w$ values were very similar for both polymers, whereas the $\bar{M}_n$ value was higher for PHO_{FD} than it was for PHO_F. As a consequence, the polydispersity index $\bar{M}_w/\bar{M}_n$ was higher for PHO_F. High molecular weights affect the flexibility of entangled polymer chains and hinder them from diffusing easily among topological obstacles coming from neighboring chains. Therefore, it restricts their ability to crystallize. However, the amorphous polymer (PHO_F) displayed a lower $\bar{M}_n$ value than the semicrystalline one (PHO_{FD}), which means that the crystallizability of PHO is not governed by its molecular weight.

Molecular weight measurements showed that the polydispersity index of PHO_F was higher than the one of PHO_{FD}. This result can be explained in terms of accessibility of the PHO granule core by sodium hypochlorite. Indeed, when bacteria are freeze-dried prior to purification, it is likely that the diffusion coefficient of sodium hypochlorite within the PHO granule is lower and that the core of the granule could remain inaccessible during the purification step. In contrast, when the bacteria are frozen, the remaining water in the granule is favorable for sodium hypochlorite diffusion into the granule core. It was shown elsewhere[18] that specific interactions between remaining sodium hypochlorite

observed for the glass transition temperature, which was found around −37 °C.

The tensile dynamic mechanical behavior of PHO films obtained from the coalescence of PHO_F granules is shown in Figure 2. No increase of the relaxed modulus with annealing time was observed, contrary to what was reported with the PHO_{FD} film.[18] Even for longer annealing times, the dynamic mechanical behavior of the PHO_F polymer did not change and displayed typical behavior of fully amorphous polymer. For temperatures below T_g the polymer was in the glassy state, and the modulus decreased slightly with temperature but remained roughly constant (around 2 GPa). Then, a rapid decrease in the elastic tensile modulus, by more than 3 orders, was observed, corresponding to the glass−rubber transition. (The rubbery modulus remains constant with time, around 1 MPa.) In the terminal zone, the elastic tensile modulus became lower with temperature, and the experimental setup failed to measure it.

To understand this peculiar phenomenon which preserved the amorphous state of PHO after particle coalescence when bacteria were frozen prior to purification, further experiments were performed. Hobbs and Barham[27] reported the effect of water on the crystallization of PHB films. They observed that the presence of water significantly enhanced the growth rate of films of PHB and P(HB-co-HV) over all temperatures up to 90 °C. They suggested that the water was acting as a
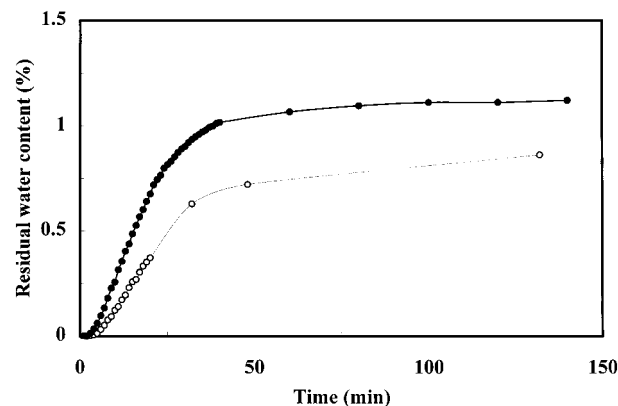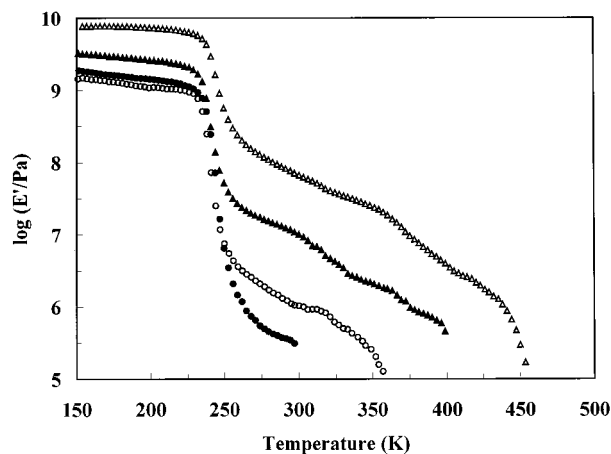
Figure 4. Reinforcing effect of starch microcrystals: logarithm of the storage tensile modulus E' versus temperature at 1 Hz for composites filled with 0 (●), 10 (○), 30 (▲), and 50 wt % (△) of starch microcrystals.

Figure 5. Reinforcing effect of tunicin whiskers: logarithm of the storage tensile modulus E' versus temperature at 1 Hz for composites filled with 0 (●), 1 (○), 3 (▲), and 6 wt % (△) of tunicin whiskers.

and PHO can lead to a slight and spontaneous cross-linking of PHO chains. The higher accessibility of the core of the frozen granule by hypochlorite could result in a slight degradation (displayed through lower $\bar{M}_n$ value) and a slight cross-linking, which could prevent any crystallization in PHO$_F$ films. Therefore, if this hypothesis is correct, the time required to treat PHO granules with hypochlorite is an important factor which can affect the crystallization of the resulting polymer.

Starch Microcrystals Filled PHO. Dynamic mechanical measurements were performed on pure PHO$_F$ matrix and up to 50 wt % starch microcrystal composites (Figure 4). For temperatures below T_g, the composite modulus increased up to 8 GPa for the 50% filled material. Above T_g a greater increase in the composite modulus was observed with an increasing volume fraction of microcrystalline starch. For instance, the relaxed modulus at $T_g + 50$ °C (~300 K) of a film containing only 30% of starch was more than 30 times higher than the PHO$_F$ matrix. For the 50% microcrystalline starch-filled composite, it was more than 200 times higher. Similar results were obtained using a synthetic copolymer of styrene and butyl acrylate as matrix.[22,23] In addition, this filler improved the temperature creep resistance of the PHO matrix.

This reinforcing effect was well described assuming a strong aggregation of filler particles and displayed two distinct regions below and above 20 vol %, which corresponded to the percolation threshold of a roughly particulate filler. As previously reported with the synthetic matrix,[23] the tensile modulus of the starch microcrystal/PHO composites was fitted using the generalized Kerner equation with an adjustable Enstein coefficient, k_E, and the Guth equation modified for nonspherical particles with an adjustable sphericity coefficient, f_g. No difference was found between the reinforcing effect of the starch microcrystal, regardless of the nature of the matrix, synthetic or bacterial (results not shown). For both systems, the k_E values were ~70 and ~400, and the f_g values were ~20 and ~40, for the low (<0.2) and high (>0.2) volume fractions, respectively.

Cellulose Microcrystals Filled PHO. Dynamic mechanical measurements were performed on a pure PHO$_F$ matrix and up to 6 wt % cellulose whisker composites (Figure 5). As reported elsewhere for a synthetic matrix,[19] the films that contained cellulose
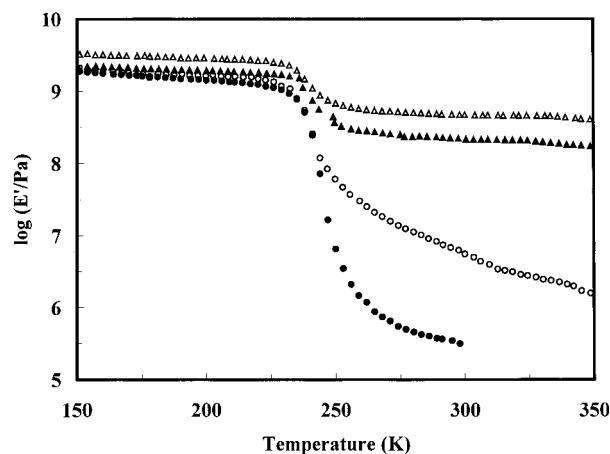
whiskers have a slight increase in their storage modulus below T_g, but the drop in E' value above T_g was dramatically reduced from 3 to 0.5 GPa for a film reinforced by 6 wt % whiskers. It was shown that this reinforcing effect strongly depended on the aspect ratio of the cellulose whisker, and therefore on its origin, as well as on the processing technique of the composite.[21,28]

The mechanical behavior of cellulose whiskers/PHO systems was predicted from a classical mean-field mechanical model developed for short fiber composites. In such an approach, following Halpin and Kardos,[29] the modulus, the mechanical anisotropy, and the geometry of the fibers are accounted for, but one assumes that there is no interactions between the fibers. In particular, the mean-field approach is based on the concept that a material made of short fibers, homogeneously dispersed in a continuous matrix, is mechanically equivalent to a superposition of four plies. Within each ply, the fibers are parallel to one another, and the mutual orientation of the plies is 0°, +45°, +90°, and −45°. The mechanical properties of each ply can be derived from the micromechanic equations of Halpin−Tsai.[30] This model is described in detail elsewhere.[19,20] The variation of the unrelaxed and relaxed tensile modulus, taken at $T_g - 50 \sim 185$ K and $T_g + 50 \sim 285$ K, respectively, is plotted as a function of the whiskers content in Figure 6, a and b, respectively. The characteristics of the fiber have the following values: $L/d = 67$ (estimated from transmission electron microscopy), Poisson's ratio = $\nu_f = 0.3$ (cellulose being in the glassy state in the whole temperature range), stiffness in the fiber direction = $E_{11f} = 150$ GPa (average value from literature),[31−36] stiffness perpendicular to the fiber direction = $E_{22f} = 15$ GPa, and in-plane shear modulus = $G_f = 5$ GPa.[36] For the matrix, the following parameters were used at 185 and 285 K, respectively: $\nu_m = 0.3$ and 0.5 (the matrix being in the glassy and rubbery state, respectively), and $E_m = 1.54$ GPa and 0.40 MPa (experimental data observed for the pure PHO matrix at 185 and 285 K, respectively). It clearly appears that the predicted modulus values agree with the experimental data in the glassy state but fail to described the rubbery modulus. The former indicates that the glassy modulus of the cellulose whiskers filled PHO is well described from a mean-field approach. The latter was previously observed for a synthetic thermoplastic matrix filled with tunicate whiskers.[19]
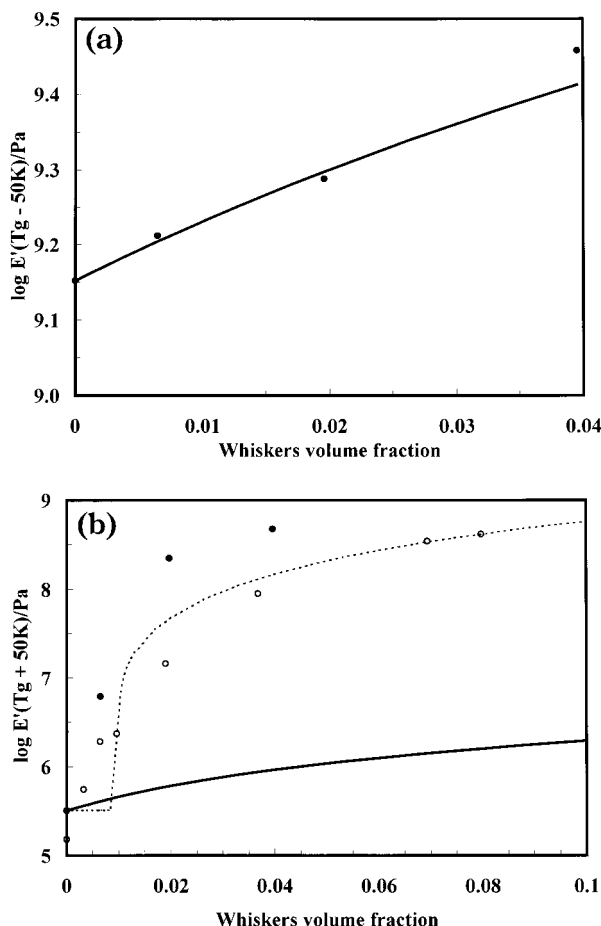
Figure 6. Reinforcing effect of tunicin whiskers: logarithm of the storage tensile modulus E' at (a, top) $T_g - 50 \sim 185$ K and (b, bottom) $T_g + 50 \sim 285$ K vs volume fraction of tunicin whiskers. Comparison between the experimental data of PHO-based systems (●) or poly(S-co-BuA)-based systems (○) (shear modulus values from ref 19 convert into tensile moduli assuming a mixture rule for the Poisson's ratio and $T_g + 50 \sim 325$ K) and predicted data from the Halpin−Kardos model (—) or from the percolation approach (- - -).

To explain the unusually high modulus values of the reinforced films, one needs to invoke (i) a strong interaction between the whiskers and (ii) a percolation effect. The influence of such an effect on the mechanical properties of the films can be calculated following the method of Ouali et al.[37] in their adaptation of the percolation concept to the classical phenomenological series−parallel model of Takayanagi et al.[38] This model was successfully used to predict the mechanical behavior of heterogeneous materials, such as polymer blends[39,40] and nanocomposite structures.[19,21,23,28] In this approach, the elastic tensile modulus E'_C of the composite is given by the following equation:

$$E'_C = \frac{(1 - 2\psi + \psi v_R)E'_S \, E'_R + (1 - v_R)\psi E'^2_C}{(1 - v_R)E'_R + (v_R - \psi)E'_S} \quad (1)$$

The subscripts S and R refer to the soft and rigid phase, respectively, and v_R corresponds to the volume fraction of filler (rigid phase). The adjustable parameter, ψ, involved in the Takayanagi et al. model corresponds in the Ouali et al. prediction to the volume fraction of the percolating rigid phase. With v_{Rc} being the critical volume fraction of the rigid phase at the percolation threshold and b the corresponding critical exponent, ψ
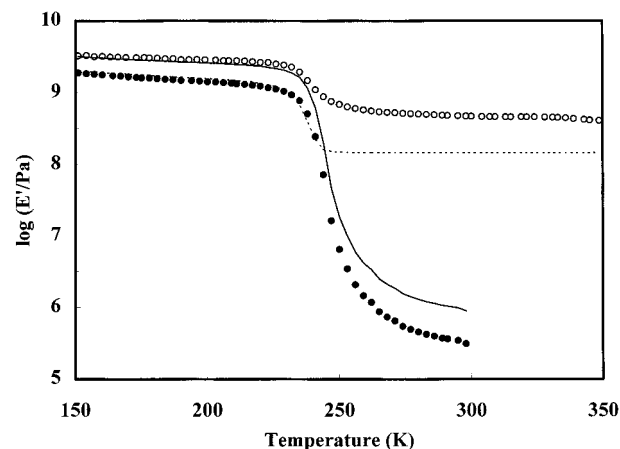

Figure 7. Reinforcing effect of tunicin whiskers: logarithm of the storage tensile modulus E' versus temperature at 1 Hz. Comparison between the experimental data for composites filled with 0 (●) and 6 wt % (○) of tunicin whiskers and predicted data from the Halpin−Kardos model (—) or from the percolation approach (- - -) for the composite filled with 6 wt % of tunicin whiskers.

can be written as

$$\psi = 0 \qquad \text{for } v_R < v_{Rc}$$

$$\psi = v_R\left(\frac{v_R - v_{Rc}}{1 - v_{Rc}}\right)^b \qquad \text{for } v_R \geq v_{Rc} \qquad (2)$$

The threshold fraction to reach percolation of whiskers was determined from a numerical calculation.[19] In our case, for tunicin whiskers, the aspect ratio is equal to 67, which leads to a very low percolation threshold close to 1 vol %, which corresponds to ∼1.5 wt % (taking 1.58 and 1.019 for the density of the filler and of the matrix, respectively). According to several studies based on the percolation concepts,[41,42] b takes the value of 0.4 in a three-dimensional system. The stiffness of the cellulose microcrystals network, different from the one of an isolated whisker, was experimentally measured from a tensile test performed on a tunicine whiskers sheet and was found equal to 15 GPa.[19] The calculated curve based on the percolation theory is reported as a dashed line in Figure 6b. The experimental data corresponding to the synthetic poly(S-co-BuA) matrix-based system obtained elsewhere[19] at $T_g + 50 \sim 325$ K are added. The calculated curve based on the percolation theory for this system is similar to the one corresponding to the natural matrix because at high temperature (i.e., above T_g) the filler modulus is far higher than the one of the matrix, and eq 1 can be simplified according to

$$E'_C = \psi E'_R \qquad (3)$$

It means that all the stiffness of the material is due to infinite aggregates of tunicin whiskers.

Figure 7 shows the plot of experimental and predicted modulus for the 6 wt % filled material over a wide temperature range. It clearly appears again that the Halpin−Kardos model agrees with experimental modulus data of the composite in the glassy state of the matrix. Neither of the two models fit the experimental data in the rubbery zone. However, the calculated curve based on the percolation concept allows to account for the stabilization of the rubbery modulus at higher whiskers loading above T_g. Indeed, the temperature

dependence of the rubbery modulus of reinforced films depended on the whiskers content (see Figure 5). Two well distinct regions are displayed depending on the concentration of whiskers. For low whiskers loading (0 and 1 wt %), the slope of the curve log E' vs temperature was around -10^{-2} K^{-1}, and it was around -10^{-3} K^{-1} for higher whiskers content (3 and 6 wt %). The differences in slope can be ascribed to the presence of strong interactions between whiskers such as hydrogen bonds, which lead to the formation of a rigid network governed by the percolation threshold. This rigid whisker network which develops above the percolation threshold by hydrogen bonding allows a thermally stable plateau to be reached. The role of percolation of cellulose fibers in paper making is well documented.[43,44] It is, in particular, established that the high mechanical properties of a paper sheet result from the hydrogen-bonding forces that hold the percolating network of the fibers. This hydrogen-bonding system is responsible for the unusual mechanical properties of the cellulose whisker-based composites when the percolation threshold is reached. Moreover, this whiskers network is also responsible for the stabilization of E' above T_g. Therefore, although mainly phenomenological, the model based on percolation concepts is able to take into account the microstructural parameters of the composites. In addition, it was reported elsewhere[28] that the reinforcing effect of particulate fillers with an aspect ratio close to 1, such as starch microcrystals, was only due to the geometrical percolation of the filler. The mechanical percolation phenomenon, which leads to higher mechanical properties through the formation of a rigid filler network, appears with increasing aspect ratio filler.

It was observed in Figure 6b that the calculated curve based on the percolation theory was lower than the solid line up to a whiskers volume fraction of $\sim$1%. The discrepancy observed between the calculated curve based on the percolation approach and the experimental data at low filler content is probably due to the fact that the prediction does not account for the distribution of the whiskers' lengths. Above this critical percentage, the calculated curve based on the percolation theory precisely fits the observed E' values when a synthetic poly-(S-*co*-BuA) was used as the matrix.[19] On the contrary, calculation underestimates the relaxed modulus of PHO-based composites. The experimental data for the PHO-based systems are 5 times higher than the predicted one. This discrepancy can ensue from three origins: (i) an inhomogeneity within the thickness of the composite because of the processing itself, the evaporation step leading to a sedimentation of the cellulose whiskers and to a multilayered material, (ii) stronger interactions between the natural PHO polyester and cellulose whiskers in comparison with the synthetic matrix, and/or (iii) a geometrical constraint due to the larger particle size of the PHO latex ($\sim$1 μm[18]) compared to the poly(S-*co*-BuA) latex ($\sim$150 nm[19]).

The former was observed for wheat straw cellulose whiskers filled poly(S-*co*-BuA) and evidenced by scanning electron microscopy (SEM), wide-angle X-ray scattering (WAXS), and dynamic mechanical analysis.[21] The behavior of these composites was well described by using a multilayered model consisting of layers parallel to the film surface.[21] To examine this sedimentation phenomenon, WAXS was used. Indeed, because of the high crystallinity level of the cellulose whiskers and the amorphous state of the polymeric matrix used, it should be possible to display the sedimentation of the filler by simply measuring and comparing the diffracted X-ray beam by the two faces of the sample. No difference was found between the two diffraction patterns (results not shown). The homogeneity of the filled samples within the thickness of the film was also confirmed by SEM observation of the fractured surface.

The two latter points (filler$-$matrix interactions and geometrical constraint due to the particle size of the latex) are more difficult to estimate experimentally. Both phenomena can be responsible for the higher mechanical properties observed with the PHO matrix. Indeed, the presence of functional groups in PHO could allow favorable interactions with the hydroxyl groups of cellulose, like hydrogen bonds. This, in turn, can result in an increase of the interfacial modulus. These specific polymer$-$filler interactions tend to create a layer of polymer surrounding each whisker, whose properties differ from those of the bulk polymer. This leads to an immobilized polymer layer (interphase) which contributes to the effective filler volume fraction in the composite. This phenomenon is assumed to be noticeable, owing to the high specific area of tunicin whiskers ($\sim$170 m^2/g). For a 6 wt % tunicin whiskers filled composite, there are of the order of 100 000 cm^2 of filler surfaces/cm^3 of material. This should have an effect on conformational properties and will certainly result in significant increases in the T_g of the matrix phase. However, the temperature position of the modulus drop associated with T_g remains almost constant, whatever the concentration of filler may be (see Figure 5). This anomalous behavior was observed elsewhere,[45,46] and based on the concept of interphase, an explanation was given by Theocaris and Spathis.[47]

In addition, the latex particle size can affect the whiskers network formation. Indeed, the particles act as impenetrable domains to whiskers during the film formation due to their high viscosity. Increasing particle size leads to an increase of the excluded volume and to a decrease of the percolation threshold.

To separate, at least qualitatively, these two effects, one can use results obtained for the starch microcrystals filled composites. In these systems and at the filler concentrations considered, there are of the order of 200 000$-$400 000 cm^2 of filler surfaces/cm^3 of material.[22] The interfacial effects should therefore be predominant, since similar interactions as those assumed with cellulose whiskers should be established with the PHO matrix, due to the similarity between cellulose and starch chemical structure and their ability to form hydrogen bonds. However, no difference was found in the previous section between the mechanical behavior of starch microcrystal filled systems using either poly-(S-*co*-BuA) or PHO as matrix. Therefore, it appears that the geometrical constraint due to the particle size of the latex seems to be the predominant phenomenon to explain the higher reinforcing effect of tunicin whiskers reported for the PHO matrix, compared to case of the synthetic poly(S-*co*-BuA) one.

Conclusion

A latex of PHO obtained from *Pseudomonas oleovorans* grown at high cell density on sodium octanoate was prepared using a chemical treatment by sodium hypochlorite. Films resulting from lattices obtained from frozen bacteria were fully amorphous. This

peculiar phenomenon, which preserves the nascent amorphous state of PHO after particle coalescence, was explained in terms of accessibility of the PHO granule core by sodium hypochlorite.

Nanocomposite materials were obtained by reinforcing amorphous PHO lattices with starch microcrystals extracted from smooth yellow pea granules or cellulose whiskers from tunicin. The mechanical properties are substantially improved by increasing the filler loading, preserving the natural and degradable nature of PHO. The reinforcing effect of polysaccharide microcrystals is strongly related to the aspect ratio of the reinforcing phase. Starch microcrystals, with an aspect ratio close to 1, display a geometrical percolation effect around 20 vol %. Tunicin whiskers, with a higher aspect ratio close to 67 and a percolation threshold close to 1 vol %, induce a mechanical percolation phenomenon which leads to higher mechanical properties through the formation of a rigid filler network. Contrary to starch microcrystals, the reinforcing effect of cellulose whiskers depends on the nature of the latex used to form the matrix. The predominant factor to explain this phenomenon seems to be a geometrical constraint due to the particle sizes of the latex, which affects the whiskers network formation during film processing. Further studies using nanocomposite materials obtained from lattices presenting different particle sizes will be fruitful to understand the role of this geometrical constraint on the whiskers percolation phenomenon.

References and Notes

(1) Dawes, E. A.; Senior, P. J. *Adv. Microbiol. Physiol.* **1973**, *10*, 135.
(2) Erson, A. J.; Dawes, E. A. *Microbiol. Rev.* **1990**, *54*, 4, 450.
(3) Doi, Y. In *Microbial Polyesters*; VCH Publishers: New York, 1990.
(4) Preusting, H.; Nijenhuis, A.; Witholt, B. *Macromolecules* **1990**, *23*, 4220.
(5) Brandl, H.; Gross, R. A.; Lenz, R. W.; Fuller, R. C. *Appl. Environ. Microbiol.* **1988**, *54*, 1977.
(6) De Smet, M. J.; Eggink, G.; Witholt, B.; Kingma, J.; Wynberg, H. J. *J. Bacteriol.* **1988**, *154*, 870.
(7) Lageveen, R. G.; Huisman, G. W.; Preusting, H.; Ketelaar, P.; Eggink, G.; Witholt, B. *Appl. Environ. Microbiol.* **1988**, *54*, 2924.
(8) Gross, R. A.; DeMello, C.; Lenz, R. W.; Brandl, H.; Fuller, R. C. *Macromolecules* **1989**, *22*, 1106.
(9) Huisman, G. W.; DeLeeuw, O.; Eggink, G.; Witholt, B. *Appl. Environ. Microbiol.* **1989**, *55*, 1949.
(10) Gagnon, K. D.; Lenz, R. W.; Farris, R. J.; Fuller, R. C. *Rubber Chem. Technol.* **1992**, *65*, 4, 761.
(11) Gagnon, K. D.; Lenz, R. W.; Farris, R. J.; Fuller, R. C. *Macromolecules* **1992**, *25*, 3723.
(12) Gagnon, K. D.; Lenz, R. W.; Farris, R. J.; Fuller, R. C. *Polymer* **1994**, *35*, 20, 4358.
(13) Lauzier, C. A.; Monasterios, C. J.; Saracovan, I.; Marchessault, R. H.; Ramsay B. A. *Tappi J.* **1993**, *76*, 5, 71.
(14) Williamson, D. H.; Wilkinson, J. F. *J. Gen. Microbiol.* **1958**, *19*, 198.
(15) Alper, R.; Lundgren, D. G.; Marchessault, R. H.; Cote, W. A. *Biopolymers* **1963**, *1*, 545.
(16) Nutti, M. P.; de Bertoldi, M.; Lepidi, A. A. *Can. J. Microbiol.* **1972**, *18*, 1257.
(17) Dawes, E. A.; Senior, P. J. *Adv. Microbiol. Physiol.* **1973**, *10*, 135.
(18) Dufresne, A.; Samain, E. *Macromolecules* **1998**, *31*, 6426.
(19) Favier, V.; Canova, G. R.; Cavaillé, J. Y.; Chanzy, H.; Dufresne, A.; Gauthier, C. *Polym. Adv. Technol.* **1995**, *6*, 351.
(20) Helbert, W.; Cavaillé, J. Y.; Dufresne, A. *Polym. Compos.* **1996**, *17*, 4, 604.
(21) Dufresne, A.; Cavaillé, J. Y.; Helbert, W. *Polym. Compos.* **1997**, *18*, 2, 198.
(22) Dufresne, A.; Cavaillé, J. Y.; Helbert, W. *Macromolecules* **1996**, *29*, 7624.
(23) Dufresne, A.; Cavaillé, J. Y. *J. Polym. Sci., Part B: Polym. Phys.* **1998**, *36*, 2211.
(24) Gagnon, K. D.; Bain, D. B.; Lenz, R. W.; Fuller, R. C. In *Novel Biodegradable Microbial Polymers*; Dawes, E. A., Ed.; Kluwer Academic Publishers: 1990; pp 449−450,
(25) Mitchell, J.; Smith, D. M. In *Aquametry*; Interscience Publishers: New York, 1948.
(26) Swensen, R. F.; Keyworth, D. A. *Anal. Chem.* **1963**, *35*, 863.
(27) Hobbs, J. K.; Barham, P. J. *Polymer* **1997**, *38*, 15, 3879.
(28) Dufresne, A. *Recent Res. Dev. Macromol. Res.* **1998**, *3*, 455.
(29) Halpin, J. C.; Kardos, J. L. *J. Appl. Phys.* **1972**, *43*, 2235.
(30) Tsai, S. W.; Halpin, J. C.; Pagano, N. J. In *Composite Materials Workshop*; Technomic: Stanford, CT, 1969.
(31) Akurada, I.; Nukushima, Y.; Ito, T. *J. Polym. Sci.* **1962**, *57*, 651.
(32) Matsuo, M.; Sawatari, C.; Iwai, Y.; Ozaki, F. *Macromolecules* **1990**, *23*, 3266.
(33) Nishino, T.; Takano, K.; Nakamae, K. *J. Polym. Sci., Part B: Polym. Phys.* **1995**, *33*, 1647.
(34) Tashiro, K.; Kobayashi, M. *Polym. Bull.* **1985**, *14*, 213.
(35) Kroon-Batenburg, L. M. J.; Kroon, J.; Northolt, M. G. *Polym. Commun.* **1986**, *27*, 290.
(36) Tashiro, K.; Kobayashi, M. *Polymer* **1991**, *32*, 8, 1516.
(37) Ouali, N.; Cavaillé, J. Y.; Perez, J. *Plast. Rub. Compos. Process. Appl.* **1991**, *16*, 55.
(38) Takayanagi, M.; Uemura, S.; Minami, S. *J. Polym. Sci. C* **1964**, *5*, 113.
(39) Garcia-Ramirez, M.; Cavaillé, J. Y.; Dufresne, A.; Tekely, P. *J. Polym. Sci., Part B: Polym. Phys.* **1995**, *33*, 2109.
(40) Garcia-Ramirez, M.; Cavaillé, J. Y.; Dufresne, A.; Dupeyre D. *J. Appl. Polym. Sci.* **1996**, *59*, 1995.
(41) de Gennes, P. G. In *Scaling Concepts in Polymer Physics*; Cornell University Press: Ithaca, NY, 1979.
(42) Stauffer, D. In *Introduction to Percolation Theory*; Taylor and Francis: London, 1985.
(43) Batten, G. L., Jr.; Nissan, A. H. *TAPPI* **1987**, *70*, 119.
(44) Nissan, A. H.; Batten, G. L., Jr. *TAPPI* **1987**, *70*, 128.
(45) Boluk, M. Y.; Schreiber, H. P. *Polym. Compos.* **1986**, *7*, 295.
(46) Dufresne, A.; Lacabanne, C. *Polym. Compos.* **1993**, *14*, 3, 238.
(47) Theocaris, P. S.; Spathis, G. D. *J. Appl. Polym. Sci.* **1982**, *27*, 3019.